Research Article

Baicalin attenuates blood-spinal cord barrier disruption and apoptosis through PI3K/Akt signaling pathway after spinal cord injury

Rui Zhao[1, 2, 3, #], Xue Wu[1, 2, 3, #], Xue-Yuan Bi[4], Hao Yang[1, 3], Qian Zhang[1, 2, 3, *]

Graphical Abstract *Baicalin improves motor functional recovery after spinal cord injury*
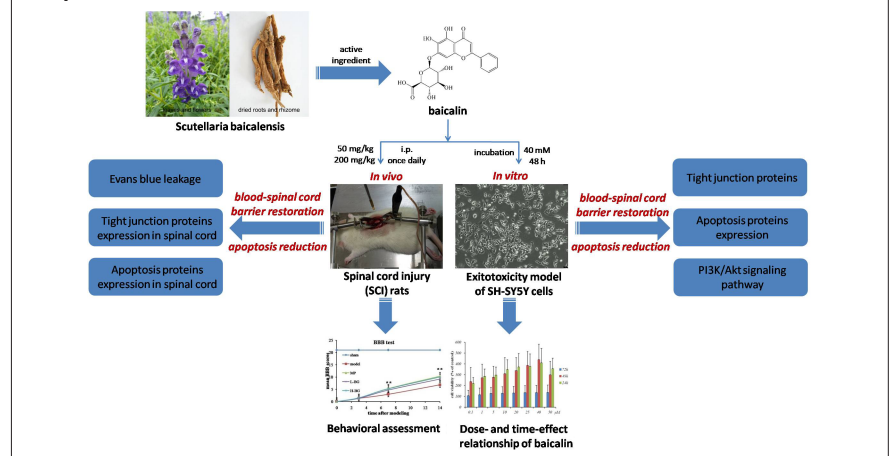
Abstract

Baicalin is a natural active ingredient isolated from Scutellariae Radix that can cross the blood-brain barrier and exhibits neuroprotective effects on multiple central nervous system diseases. However, the mechanism behind the neuroprotective effects remains unclear. In this study, rat models of spinal cord injury were established using a modified Allen's impact method and then treated with intraperitoneal injection of Baicalin. The results revealed that Baicalin greatly increased the Basso, Beattie, Bresnahan Locomotor Rating Scale score, reduced blood-spinal cord barrier permeability, decreased the expression of Bax, Caspase-3, and nuclear factor κB, increased the expression of Bcl-2, and reduced neuronal apoptosis and pathological spinal cord injury. SH-SY5Y cell models of excitotoxicity were established by application of 10 mM glutamate for 12 hours and then treated with 40 µM Baicalin for 48 hours to investigate the mechanism of action of Baicalin. The results showed that Baicalin reversed tight junction protein expression tendencies (occludin and ZO-1) and apoptosis-related protein expression (Bax, Bcl-2, Caspase-3, and nuclear factor-κB), and also led to up-regulation of PI3K and Akt phosphorylation. These effects on Bax, Bcl-2, and Caspase-3 were blocked by pretreatment with the PI3K inhibitor LY294002. These findings suggest that Baicalin can inhibit blood-spinal cord barrier permeability after spinal cord injury and reduce neuronal apoptosis, possibly by activating the PI3K/Akt signaling pathway. This study was approved by Animal Ethics Committee of Xi'an Jiaotong University on March 6, 2014.

Key Words: apoptosis; baicalin; blood-spinal cord barrier; natural products; neuron; PI3K/Akt signaling pathway; spinal cord injury; tight junction

Chinese Library Classification No. R453; R744; R284

Introduction

Spinal cord injury (SCI) is a severe event with high morbidity and severe complications. In addition to conventional surgery, the most common treatment is administration of glucocorticoids (Ahuja et al., 2017). However, glucocorticoids are controversial because of their wide range of unintended side effect, which has pushed the need to discovering new drugs (Brotfain et al., 2016).

In the pathological process of secondary injury after SCI, the blood-spinal cord barrier (BSCB) plays an important role (Koehn, 2020; Ye et al., 2021). As a specialized physical barrier, the BSCB controls the exchange of substances between

[1]College of Pharmacy, Shaanxi University of Chinese Medicine, Xi'an, Shaanxi Province, China; [2]Key Laboratory of the Ministry of Education for Medicinal Resources and Natural Pharmaceutical Chemistry, National Engineering Laboratory for Resource Development of Endangered Crude Drugs in Northwest China, College of Life Sciences, Shaanxi Normal University, Xi'an, Shaanxi Province, China; [3]Translational Medicine Center, Hong Hui Hospital, Xi'an Jiaotong University, Xi'an, Shaanxi Province, China; [4]Department of Pharmacy, Hong Hui Hospital, Xi'an Jiaotong University, Xi'an, Shaanxi Province, China

*Correspondence to: Qian Zhang, PhD, zq-melody@163.com.

https://orcid.org/0000-0002-3859-6503 (Qian Zhang)

#Both authors contributed equally to the work.

the blood and the spinal cord. It blocks the entry of foreign molecules and maintains homeostasis of the spinal cord parenchyma (Bartanusz et al., 2011; Quadri et al., 2020). At the molecular level, the protective function of BSCB has been attributed to its intricate combination of multiple proteins, especially tight junction (TJ) proteins and adherens junction proteins (Coisne and Engelhardt, 2011; Kumar et al., 2017). After SCI, numerous blood-derived leukocytes invade the spinal cord parenchyma, which induces increases in matrix metalloproteinases and pro-inflammatory cytokines such as tumor necrosis factor-α and interleukin (IL)-1β, which promptly activates microglia and astrocytes. The activated microglia and astrocytes, in turn, secrete more pro-inflammatory cytokines, matrix metalloproteinases, and reactive oxygen. These factors are damaging and induce neuroinflammatory responses and oxidative stress injury, which are toxic to neurons and induce apoptosis (Wu et al., 2003; Sandhir et al., 2011; Lee et al., 2012; Ozturk et al., 2018). Therefore, therapies or drugs that target these processes (BSCB disruption and apoptosis) could be promising alternative treatments for SCI.

Baicalin (BG; 5,6-dihydroxy-4-oxygen-2-phenyl-4H-1-benzopyran-7-beta-D-glucopyranose acid; $C_{21}H_{18}O_{11}$) is one of the most important flavonoid compounds isolated from Scutellariae Radix, which is the radix (root) of Scutellaria baicalensis Georgi. In Chinese Pharmacopoeia (2020 edition), BG is specified for quality control of Scutellariae Radix and its content should not be less than 9% (China Pharmacopoeia Commission, 2020). BG possesses various pharmacological properties. In particular, it can facilitate neuronal differentiation and inhibit neuronal apoptosis, as well as alleviate neuroinflammation in the central nervous system (CNS) (Li et al., 2018, 2020; Jin et al., 2019). Most importantly, it can freely cross the blood-brain barrier and provides neuroprotection in a variety of CNS diseases (Fang et al., 2018; Zhang et al., 2018; Liu et al., 2020). This property of BG overcomes the low bioavailability of most drugs targeting the CNS, and thus has a great advantage in treating CNS diseases (Sowndhararajan et al., 2018).

The current study investigated the effectiveness of BG in treating SCI *in vivo* and *in vitro*, as well as the mechanism underlying its effects. Its neuroprotective effects and therapeutic action were studied in a rat model of SCI. Specifically, we measured motor function recovery and BSCB permeability. The mechanism through which BG affects BSCB restoration and neuronal apoptosis was investigated by focusing on the changes in expression of TJ and apoptosis-related proteins, as well as activation of the phosphatidylinositol 3-kinase/protein kinase B (PI3K/Akt) signaling pathway.

Materials and Methods
Animals and experimental design
One hundred and twenty specific-pathogen-free female Sprague-Dawley rats (12 weeks old, weight 200 ± 20 g) were purchased from the Experimental Animal Center of Xi'an Jiaotong University (approval No. SCXK [Shaanxi] 2007-001). Because estrogen has been reported to provide neuroprotection and decrease mortality rate, only female rats were used. Rats were housed in standard conditions: 22 ± 2°C, 12-hour dark/light cycle, and free access to food and water. Animal study was conducted according to the Care and Use of Laboratory Animals Guide and approved by the Animal Ethics Committee of Xi'an Jiaotong University on March 6, 2014.

For the experiments, 120 rats were randomly divided into five groups (*n* = 24/group): sham, SCI, methylprednisolon (MP), low-dose BG (SCI + 50 mg/kg BG), and high-dose BG groups (SCI + 200 mg/kg BG).

SCI model establishment and drug administration
SCI models were established using a modified Allen's method as described previously (Zhang et al., 2019). Briefly, rats were anesthetized by intraperitoneal administration of pentobarbital sodium (40 mg/kg; Sigma, St. Louis, MO, USA; Cat# P3761). A laminectomy was performed at spinal cord levels T9–10, exposing spinal cord. While clamping the spine, a moderate contusion was induced using a device (RWD G124-138; RWD, Shenzhen, China) that dropped a 10 g rod from a height of 50 mm onto the exposed cord. After surgery, the bladders of the model rats were evacuated twice daily, and gentamicin (80,000 U/rat, via intramuscular injection; Sigma, Cat# G3632) was administered. In the sham group, rats underwent anesthesia, skin incision, and laminectomy, but without dural compression. BG was purchased from Aladdin Co., Ltd. (Shanghai, China; lot No. B110211, CAS No. 21967-41-9). It was dissolved in saline containing 0.5% poloxamer and administered to rats once daily from the day of surgery (50 or 200 mg/kg, intraperitoneal injection) until sacrifice. A vehicle solution (0.9% normal saline; 2 mL) was administered to rats in sham and SCI groups by gavage once per day. Injectable MP (SOLU-MEDROL®) was purchased from Pfizer Manufacturing Belgium NV (Rijksweg, Belgium; license No. H20130301) and used as a drug treatment comparison. Because MP is commonly used in the clinical treatment of SCI, we included an MP group that received MP via the caudal veins 30 minutes after surgery (30 mg/kg), referring to clinical dosage (Ahuja et al., 2017).

Behavioral assessment
According to the Basso, Beattie, and Bresnahan (BBB) Locomotor Rating Scase (Basso et al., 1995), limb movement, gait, coordination and paw placement were evaluated 0, 3, 7, and 14 days after surgery (*n* = 6 rats/group). Evaluations were on a scale from 0 (flat paralysis) to 21 (normal gait), and were conducted independently by two researchers who were blinded to experimental groupings.

Tissue collecting and processing
Eighteen rats in each group were sacrificed by intraperitoneal administration of pentobarbital sodium (40 mg/kg) to collect spinal cords 3 days after SCI. Among them, six were used for BSCB permeability evaluation; six for immunohistochemical assay and *in situ* TdT-mediated dUTP nick end-labeling (TUNEL) assay; and six for western blot assay.

For the immunohistochemical and TUNEL assay, rats were transcardially perfused with normal saline (100 mL) and 4% paraformaldehyde (100 mL) in sequence after anesthesia. Spinal cords were put in 4% paraformaldehyde overnight, and then successive 20% and 30% sucrose solutions. Then, 20-mm lengths of spinal cord with the epicenter at the center were embedded in an optimal cutting temperature compound (Sakura Finetek, Torrance, CA, USA; Cat# 4583) and cut into sections (14 μm) with a freezing microtome (Leica, Wetzlar, Germany). For the western blot assay, spinal cords were freshly collected without perfusion, and frozen at –20°C for use. For the BSCB permeability measurement, spinal cords were freshly collected.

Measurement of Evans blue leakage
Extravasation of Evans blue (EB) in the spinal cord can be used to quantitatively evaluate BSCB permeability. Briefly, 3 days post-surgery, rats were deeply anesthetized with pentobarbital sodium (40 mg/kg) and EB solution (45 mg/kg) was injected into caudal vein. After EB circulated in the body for 30 minutes, rats rwere transcardially perfused with normal saline until colorless saline outflowed from the right atrium. Spinal cords were harvested, weighed accurately, and cut into pieces. Twofold volume of formamide was added to

homogenate of the spinal cord (1 mL/100 mg) and placed in a water bath at 45°C for 48 hours. After centrifuging at 1006.2 × *g* for 10 minutes, the supernatant was transferred and determined by spectrophotometry (Thermo Fisher, Waltham, MA, USA) at 620 nm. The quantitative calculation of EB dye content in spinal cord tissue was based on external standards dissolved in the same solvent.

Immunohistochemical assay and TUNEL assay

For immunohistochemical staining, after incubating in goat serum for 60 minutes, sections were incubated with rabbit monoclonal anti-occludin antibody (1:200; Abcam, Cambridge, UK; Cat# ab216327) and rabbit polyclonal anti-zonula occluden-1 (ZO-1) antibody (1:200; Proteintech, Rosemont, IL, USA; Cat# 21773-1-AP) at 4°C overnight. After washing, goat anti-rabbit horseradish peroxidase secondary antibody (1:5000; Boster, Wuhan, China; Cat# BA1054) was applied at room temperature for 1 hour. The signal was visualized with 3,3′-diaminobenzidine (Boster; Cat# AR1022) chromogen under a light microscope (DM1000; Leica). Lastly, sections were counterstained with hematoxylin, rinsed by tap water, and photographed.

For the apoptosis assay, sections were first incubated with goat polyclonal anti-tubulin-3 (1:200; Bioss, Beijing, China) at 4°C overnight. After washing, sections were incubated with rabbit anti-goat secondary antibody (1:200, fluorescein isothiocyanate (FITC); Boster; Cat# BA1110) for 1 hour at room temperature. With regard to TUNEL staining, TUNEL mixture (*in situ* cell apoptosis detection kit IV, Cy3; Boster) was used for staining at 37°C for 1 hour. Then, glass slides were covered with 4′,6-diamidino-2-phenylindole (1:2000; BD, Franklin Lakes, NJ, USA) for 5 minutes, washed three times, and immediately photographed under a fluorescence microscope (DM1000; Leica).

Finally, ImageJ (National Institutes of Health, Bethesda, MD, USA) was used for semi-quantitative analysis using the sum of the integrated optical density (IOD) values. From each group, six representative visual fields were chosen to calculate the IOD, which equaled the optical density divided by the neutral area in the immunohistochemical image.

Western blot assay

Total protein was extracted from spinal cord tissues or cells. After heating at 95°C for 5 minutes, 30 mg of protein sample was separated by sodium dodecyl sulfate-polyacrylamide gel electrophoresis with 12% (Bcl-2, Bax and Caspase-3), 10% (occludin and nuclear factor-κB [NF-κB] p65) or 8% (ZO-1) gels. Protein bands were electroblotted onto polyvinylidene difluoride membranes and blocked with non-fat dried milk for 1 hour. The blots were then probed with rabbit anti-occludin monoclonal antibody (1:1000; Abcam, Cat# ab216327), rabbit anti-ZO-1 polyclonal antibody (1:1000; Proteintech, Cat# 21773-1-AP), rabbit anti-Bcl-2 polyclonal antibody (1:1000; Bioss, Cat# bs-0032R), rabbit anti-Bax polyclonal antibody (1:1000; Bioss, Cat# bs-0127R), rabbit anti-Caspase-3 polyclonal antibody (1:1000; Bioss, Cat# bs-0081R), rabbit anti-NF-κB p65 monoclonal antibody (1:1000; Cell Signaling Technology, Danvers, MA, USA; Cat# 8242), rabbit anti-pan-PI3K polyclonal antibody (1:1000; Affinity, Cincinnati, OH, Cat# AF6241), rabbit anti-p-PI3K polyclonal antibody (1:1000; Affinity, Cat# AF3241), rabbit anti-pan-AKT polyclonal antibody (1:1000; Affinity, Cat# AF6261), and rabbit anti-p-AKT polyclonal antibody (1:1000; Affinity, Cat# AF0016) overnight at room temperature. After washing with Tris buffered saline with Tween®, sections were incubated with peroxidase anti-rabbit IgG (1:5000; Boster; Cat# BA1054) secondary antibodies for 1 hour at room temperature. Immunoreactivity was detected by enhanced chemiluminescence assay. Autoradiograms were exposed for 5–15 minutes. The micrographs were analyzed by ImageJ. After defining a threshold for background correction, the relative optical densities of occludin, ZO-1, Bcl-2, Bax, Caspase-3, and NF-κB with β-actin (1:200; Boster, Cat# BM0627; mouse, monoclonal antibody) in the spinal cord and primary cultured cells were calculated.

Cell culture and drug intervention

The SH-SY5Y cell line was purchased from Shanghai Institute of Biochemistry and Cell Biology (Shanghai, China). Cells were cultured in a minimum essential medium/Ham's F12 (MEM/F12) complete medium composed of 43.5% MEM medium (Invitrogen, USA), 43.5% F12 medium (Invitrogen), 10% fetal bovine serum (Gibco, Life Technologies, Monza, IT, USA), 1% GlutaMAX™ (Invitrogen), 1% sodium pyruvate (Invitrogen), and 1% non-essential amino acid (Invitrogen) at 37°C in an air atmosphere containing 95% air and 5% CO_2 with a saturated humidity. Upon a confluence of 60–70%, SH-SY5Y cells were divided into: (i) control cells, which were incubated in MEM/F12 complete medium without other treatment; (ii) model cells, which were subjected to glutamate (Glu; 10 mM, 12 hours; Solarbio, Beijing, China) induction; (iii) BG-treated cells, which were treated with BG (40 μM, 48 hours) 12 hours after Glu application; and (iv) cells treated with BG and LY294002, which were incubated with LY294002 (10 μM, 12 hours; Med Chem Express, NJ, USA; Cat# HY-10108), and then treated with BG after Glu application.

Cell viability assay

Cell viability was assayed using cell counting kit-8. Various concentrations and incubation times of Glu (0.01, 0.05, 0.1, 0.5, 1, 5, 10, 50, 100 mM for 12 and 1 hour) and BG (0.1, 1, 5, 10, 20, 25, 40, 50 μM for 24, 48, 72 hours) were selected to treat cells in a 96-well plate. Cell counting kit-8 reagent (10 μL; Boster, Cat# AR1160-500) was added to the 96-well plate and cultured in a cell incubator for 1 hour. Then, optical density was measured with a microplate reader (Thermo Fisher Scientific, Waltham, MA, USA) at 450 nm. All experiments were performed in triplicate. Cell viability was calculated as follows: cell viability (%) = (drug wells − blank wells) / (control wells − blank wells) × 100.

Immunofluorescence assay

The immunofluorescence assay was conducted to stain TJ proteins in SH-SY5Y cells. Glass sheets were coated with 100 μg/mL poly-L-lysine (Sigma) for 4 hours, then washed with sterile water three times and dried for later use. SH-SY5Y cell suspension was seeded on the coated-glass sheets. For immunofluorescence staining, after washing with phosphate-buffered saline, the glass sheets were incubated with rabbit polyclonal anti-occludin (1:200; Abcam, Cat# ab216327) and rabbit polyclonal anti-ZO-1 antibody (1:200; Proteintech, Cat# 21773-1-AP) at 4°C overnight. After washing with phosphate-buffered saline, the glass sheets were incubated with goat anti-rabbit FITC secondary antibody (1:200; Boster, Cat# BA1105) for 1 hour at room temperature. Subsequently, they were covered with 4′,6-diamidino-2-phenylindole (Boster, Cat# AR1176) for 5 minutes at room temperature, washed three times with phosphate-buffered saline, and placed on glass slides with cells fixed. The labeled sections were immediately observed under a fluorescence microscope (DM1000; Leica).

ImageJ was used for semi-quantitative analysis of the IOD values using the same method that we employed in the immunohistochemical assay.

Statistical analysis

All results are expressed as mean ± standard deviation (SD). Statistical differences were analyzed with one-way analysis of variance followed by the least significant difference *post hoc* test (SPSS 22; IBM Co., Armonk, NY, USA). A *P*-value < 0.05 was considered statistically significant.

Results

BG promotes motor function recovery in SCI rats

The procedure for generating SCI model rats is shown in **Figure 1A**. After striking the spinal cord, a visible edema and hemorrhage occurred within a few seconds (**Figure 1B**). After SCI, both motor and bladder functions exhibited significant defects. Specifically, no observable hindlimb movement was observed in SCI, MP, or low- and high-dose BG groups, all of which had BBB scores of 0 on the day of surgery (**Figure 1C**). Among the rats, two joints, two hips, and two knees were irresponsive, and posterior limbs could only drag on the floor. At the same time, because SCI rats lost the ability to urinate by themselves, soft bladder compression manually twice a day was necessary to prevent uroschesis. From days 7 to 14, BBB scores indicated that administration of both low-dose and high-dose BG significantly relieved motor disturbances in the posterior limb ($P < 0.01$, *vs*. SCI group). The effect of high-dose BG was equivalent to that of MP treatment ($P = 1.000$).

BG decreases BSCB permeability in SCI rats

After harvesting spinal cords 3 days post-injury, EB solution was injected into the caudal veins of all rats. As showed in **Figure 1D**, eyes, ears, paws, and tails of the SCI rats turned blue within 10 seconds after EB injection. This phenomenon indicated that EB dye was distributed to the whole body through the blood vascular system in a very short time. After 30 minutes of circulation, the spinal cord and the surrounding muscle tissue were clearly dyed blue in the SCI, MP, and BG groups. This was in sharp contrast with the clear white spinal cord and pink muscle tissue before EB injection (**Figure 1E**).

In the sham group, although vertebral lamina at spinal cord levels T9–10 was removed in SCI surgery, no strike was conducted and the BSCB remained relatively intact. Thus, most of the EB was hindered by the physical barrier and only a small amount was detected in the spinal cord tissues 3 days after surgery. In contrast, the BSCB of rats in the SCI, MP and BG groups was damaged by the weight-drop, which resulted in a significant increase in spinal cord EB content 3 days after SCI ($P < 0.05$, *vs*. sham group). However, compared with the SCI group, intraperitoneal injection of BG for 3 consecutive days, resulted in significantly less EB content for both the low- and high-dose BG groups ($P < 0.01$, *vs*. SCI group; **Figure 1F**). The effects of low- and high-dose BG were comparable with those of MP. This result indicated that BG (50 or 200 mg/kg) could decrease the permeability of destroyed BSCB, which was helpful for SCI recovery.

BG increases TJ proteins in the spinal cord after SCI

Changes in protein expression levels for TJ proteins (occludin and ZO-1) were evaluated by immunohistochemical assay and western blot 3 days after SCI. IOD values showed that TJ protein expression in gray matter of the spinal cord tissue was significantly less after SCI ($P < 0.01$, *vs*. sham group). Reduced occludin expression was significantly recovered both by low-dose and high-dose BG administration ($P < 0.01$, *vs*. SCI group). However, BG did not counter the change in ZO-1 expression ($P = 0.168$ and 0.534, respectively for low-dose and high-dose BG groups *vs*. SCI group; **Figure 2A** and **B**). Western blot results confirmed these finding.

BG reduces apoptosis in the spinal cord after SCI

Neuronal apoptosis was assessed 3 days post-SCI. TUNEL and tubulin-3 were co-labeled in spinal cord sections. While the sham group exhibited little neuronal apoptosis, injured rats exhibited significantly more neuronal apoptosis (labeled red by Cy3 in **Figure 3A**). Compared with the SCI group, administering MP or BG resulted in significantly fewer numbers of neurons positively labeled by TUNEL ($P < 0.01$). The effect of high-dose

BG was equivalent to that of MP ($P = 0.598$, **Figure 3B**).

Expression levels of apoptosis-related proteins in the spinal cord were also measured by western blot assay 3 days after SCI. We found that the IODs for Caspase-3, NF-κB, and Bax were significantly greater after injury, while Bcl-2 levels were significantly lower (All $P_s < 0.01$, *vs*. sham group). After 3 continuous days of BG treatment, these trends were completely reversed ($P < 0.01$, *vs*. SCI group). The effect of BG on the expression of these important apoptosis-associated proteins was equivalent to that of MP (**Figure 2C** and **D**).

BG increases cell viability of SH-SY5Y cells

Appropriate concentrations and time points for Glu and BG were determined according to the results of the cell-viability assay. Nine concentrations (0.01, 0.05, 0.1, 0.5, 1, 5, 10, 50, and 100 mM) and two time points (12 and 1 hour) were assayed for excitotoxicity. As shown in **Figure 4A**, following exposure to Glu for 12 hours, cell viabilities at all concentrations were below 100%, and compared with the control group, cell viability decreased by half at 10 mM Glu. In contrast, following exposure to Glu for 1 hour, although cell viability declined along with increased Glu concentrations, the numeric values were still above 100% at the concentration range of 0.01–5 mM. Therefore, 10 mM and 12 hours were selected for the excitotoxicity model using SH-SY5Y cells.

BG was used to treat SH-SY5Y cells after building the excitotoxicity model with Glu. Cell viability was assayed under eight BG concentrations (0.1, 1, 5, 10, 20, 25, 40, 50 μM) and three time points (24, 48, 72 hours). As shown in **Figure 4B**, cell viability was significantly higher at 48 and 72 hours than at 24 hours. Meanwhile, cell viability gradually increased with BG concentration, and reached a peak at 40 μM. Therefore, 40 μM and 48 hours were selected as appropriate concentration and treatment time to analyze the effects of BG on the excitotoxicity model of SH-SY5Y cells.

SH-SY5Y control cells in normal conditions possess typical epithelioid cell morphology. After treatment with Glu, the vast majority of cells shrunk and became round in shape. In the BG-treated cells, excitotoxicity caused by Glu was alleviated and cell morphology was similar to that of the control cells. In the cells treated with BG and LY294002, the cell morphology was an intermediate between what was observed in the Glu-treated and BG-treated cells (**Figure 4C**).

BG attenuates the destruction of junction proteins in the excitotoxicity model of SH-SY5Y cells

In the control cells, green fluorescence of TJ proteins was observed in cell membranes, which looked like many loops gathered together. After treating with 10 mM Glu for 12 hours, most of the annular morphology of green fluorescence disappeared because of the Glu-induced excitotoxicity. However, in the cells treated with BG, cell injury was greatly alleviated (40 μM, 48 hours), as evidenced by the undisturbed annular green fluorescence (**Figure 5A** and **B**). These changes were verified by analysis of the IODs for occludin and ZO-1 (**Figure 5C**).

Western blot results also confirmed these findings. BG treatment significantly rescued the reduction in occludin and ZO-1 expression that was observed in Glu-treated SH-SY5Y cells. Additionally, this effect was blocked by the PI3K inhibitor LY294002 ($P < 0.01$, *vs*. BG group; **Figure 6A** and **B**). However, it is worth noting that western blot results for TJ proteins in SH-SY5Y cells did not completely coincide with that in the SCI model rats; in spinal cord tissue, rescue of BG on ZO-1 expression was not significant ($P = 0.091$ and 0.186, respectively for the low-dose and high-dose BG groups *vs*. SCI group, *vs*. SCI group; **Figure 2C** and **D**).
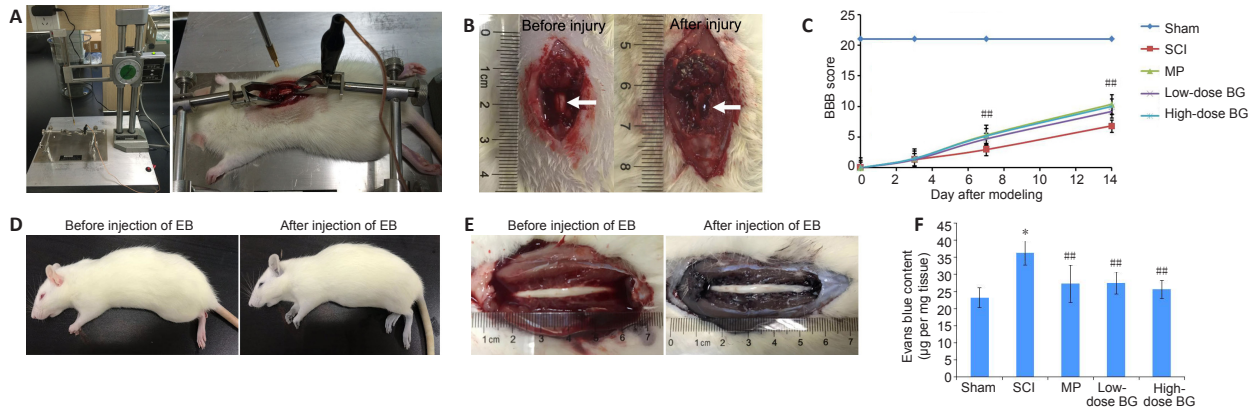
Figure 1 | Effects of BG on motor function and BSCB permeability in a rat model of SCI.
(A) The weight-drop device and the process of creating the SCI model. (B) Photograph of exposed spinal cord before and after contusion injury induced by the weight-drop device. Hemorrhages and edema are clearly observed in the spinal cord after contusion (labeled with white arrows), compared with spinal cord without injury. (C) Effect of BG on motor function, as assessed using the BBB locomotor scale up to 14 days after SCI. (D) Photograph of rats before and 30 minutes after caudal vein injection of EB. Eyes, ears, paws, and tails of rats turn blue after injection of EB. (E) Photograph of exposed spinal cord before and 30 minutes after caudal vein injection of EB. The surrounding spinal cord and muscle tissue have been dyed blue by EB. (F) Quantified EB content 3 days after SCI. Data are presented as mean ± SD (n = 6 per group). *P < 0.05, $vs.$ sham group; ##P < 0.01, $vs.$ SCI group (one-way analysis of variance followed by the least significant difference $post hoc$ test). BBB: Basso, Beattie, and Bresnahan; BG: baicalin; BSCB: blood-spinal cord barrier; EB: Evans blue; MP: methylprednisolone; SCI: spinal cord injury.
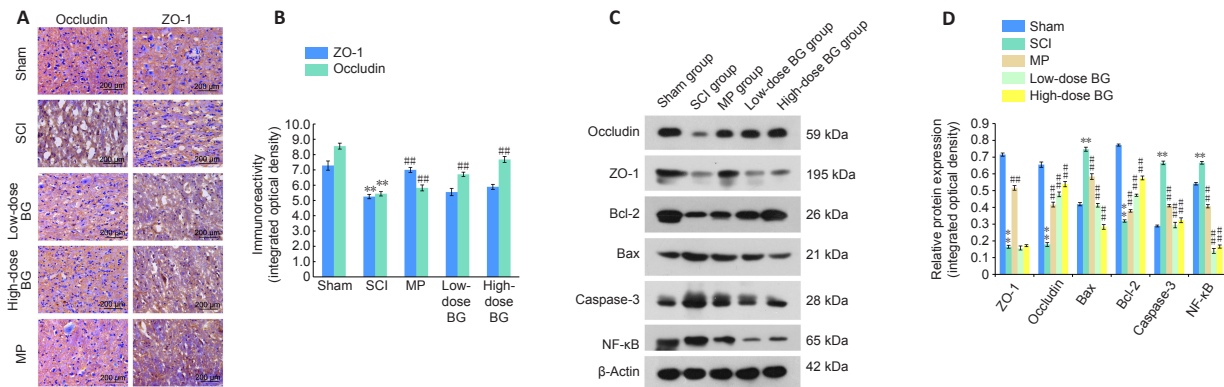
Figure 2 | Effect of BG on tight junction and apoptosis proteins in rat spinal cord 3 days after SCI.
(A) Immunohistochemical staining of tight junction proteins (occludin and ZO-1). Occludin expression was significantly lower than controls after SCI, but was at normal levels after treatment with MP, low-dose BG, and high-dose BG. Scale bars: 200 μm. (B) Quantitative analysis of integrated optical density for occludin and ZO-1. (C) Western blot assay of tight junction (occludin, ZO-1) and apoptosis (Bcl-2, Bax, Caspase-3, NF-κB) proteins. (D) Quantitative analysis of protein expression for occludin, ZO-1, Bcl-2, Bax, Caspase-3, and NF-κB. Data are presented as mean ± SD (n = 6 per group). **P < 0.01, $vs.$ sham group; ##P < 0.01, $vs.$ SCI group (one-way analysis of variance followed by the least significant difference $post hoc$ test). BG: Baicalin; MP: methylprednisolone; NF-κB: nuclear factor-κB; SCI: spinal cord injury; ZO-1: zonula occluden-1.
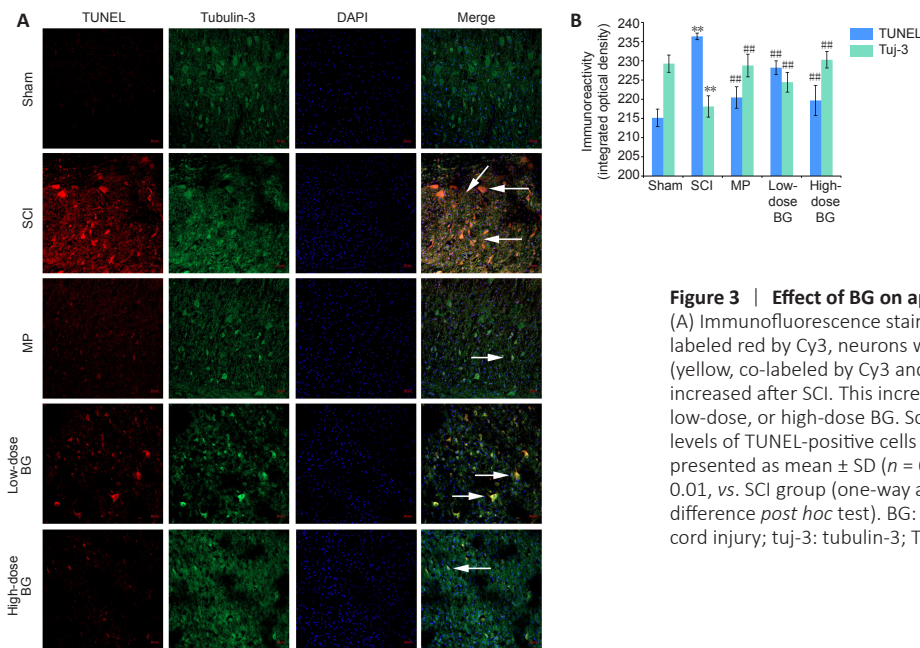
Figure 3 | Effect of BG on apoptosis in the spinal cord of the rat model of SCI.
(A) Immunofluorescence staining of TUNEL-positive neurons. TUNEL cells were labeled red by Cy3, neurons were labeled green by FITC. Neuronal apoptosis (yellow, co-labeled by Cy3 and FITC; indicated by white arrows) significantly increased after SCI. This increase was significantly less after administration of MP, low-dose, or high-dose BG. Scale bars: 50 μm. (B) Quantitative analysis of relative levels of TUNEL-positive cells and positive neurons (tuj-3 positive cells). Data are presented as mean ± SD (n = 6 per group). **P < 0.01, $vs.$ sham group; ##P < 0.01, $vs.$ SCI group (one-way analysis of variance followed by the least significant difference $post hoc$ test). BG: Baicalin; FITC: fluorescein isothiocyanate; SCI: spinal cord injury; tuj-3: tubulin-3; TUNEL: $in situ$ TdT-mediated dUTP nick end labeling.
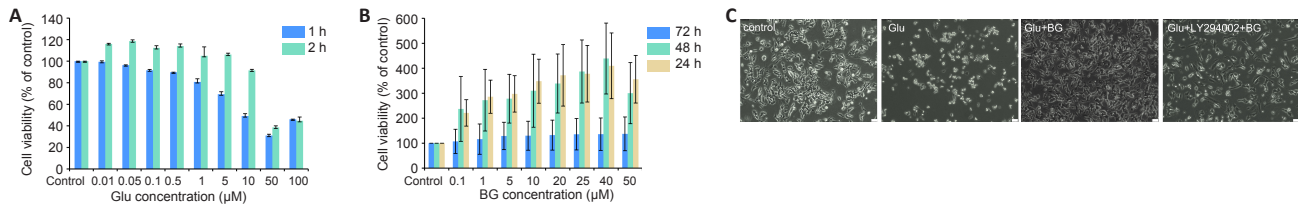
Figure 4 │ Dose-effect and time-effect relationship of glutamate (Glu) and BG on cell viability of SH-SY5Y cells.
(A) Cell viability after treating with different concentrations of Glu and for different incubation times. (B) Cell viability of SH-SY5Y cells with excitotoxicity damage after treating with BG at different concentrations and incubation times. Data are presented as mean ± SD, and were analyzed by one-way analysis of variance followed by the least significant difference *post hoc* test. The experiment was repeated three times. (C) Cell morphology of SH-SY5Y cells. Epithelioid cell morphology of SH-SY5 disappears after incubation with Glu (10 mM, 12 hours), most cells shrink and become round. After additional incubation with BG (40 μM, 48 hours), cell morphology is recovered. Scale bars: 25 μm. BG: Baicalin; LY: LY294002, an inhibitor of PI3K.
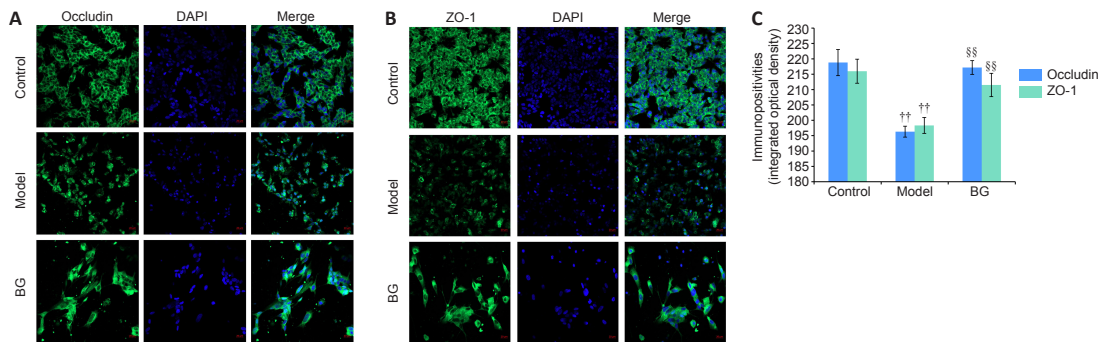
Figure 5 │ Effect of BG on tight junction protein in SH-SY5Y cells.
(A, B) Immunofluorescence staining of occludin (green, FITC) and ZO-1 (green, FITC). Annular morphology is destroyed after incubation with Glutamate (10 mM, 12 hours). After incubation with BG (40 μM, 48 hours), cell injury was greatly alleviated and annular green fluorescence is visible. Scale bars: 20 μm. (C) Quantitative analysis of immunopositivities of occludin and ZO-1. Data are presented as mean ± SD. The experiment was repeated three times. ††*P* < 0.01, *vs.* control group; §§*P* < 0.01, *vs.* model group (one-way analysis of variance followed by the least significant difference *post hoc* test). BG: Baicalin; DAPI: 4',6-diamidino-2-phenylindole; FITC: fluorescein isothiocyanate; LY: LY294002, an inhibitor of PI3K; ZO-1: zonula occluden-1.

BG inhibits expression of apoptosis-related proteins through the PI3K/Akt pathway in SH-SY5Y cells

Expression of apoptosis-related proteins in the excitotoxicity model of SH-SY5Y cells was measured by western blot assay. Expression levels of Caspase-3, NF-κB, and Bax were significantly higher in the Glu-treated cells than in control cells, while Bcl-2 expression was significantly lower (*P* < 0.01, *vs.* control cells; **Figure 6A** and **B**). After incubation with BG (40 μM, 48 hours), these trends were completely reversed (*P* < 0.01, *vs.* model cells; **Figure 6A** and **B**). Furthermore, these effects on Caspase-3, Bax, and Bcl-2 were blocked by LY294002 (*P* < 0.01, *vs.* BG-treated cells; **Figure 6A** and **B**), while no blockage effect was observed for NF-κB.

We next focused on the effect of BG on the PI3K/Akt pathway in the excitotoxicity model. Expressions of pan-PI3K and pan-Akt did not change appreciably after treating with BG (*P* = 0.857 and 0.926, respectively for BG-treated cells *vs.* model cells; **Figure 6C** and **D**) or BG + LY294002 (*P* = 0.593 and 0.780, respectively for BG-treated cells with LY294002 *vs.* BG-treated cells; **Figure 6C** and **D**). However, expressions of p-PI3K, p-Akt, p/pan-PI3K, and p/pan-Akt were significantly less in the Glu-treated model cells than in the control cells (*P* < 0.01). After treating the model cells with BG (40 μM, 48 hours), this change was reversed (*P* < 0.01, *vs.* model cells; **Figure 6C** and **D**). Again, this rescue effect was blocked by LY294002 (*P* < 0.01, *vs.* BG group; **Figure 6C** and **D**).
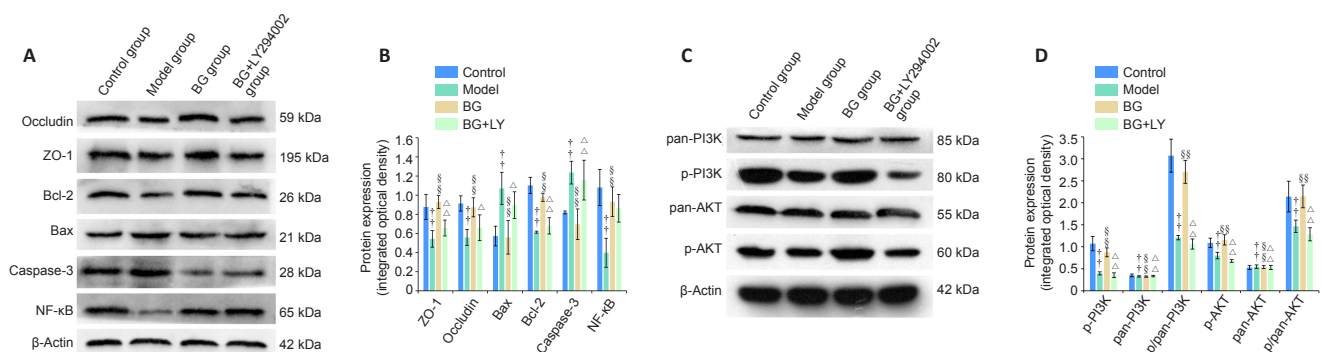
Figure 6 │ Effect of BG on PI3K/Akt signaling with respect to restoring the blood-spinal cord barrier and to anti-apoptosis in SH-SY5Y cells.
(A, B) Western blot assay and quantitative analysis of integrated optical densities for tight junction (occludin, ZO-1) and apoptosis-related (Bcl-2, Bax, Caspase-3, NF-κB) proteins. (C, D) Western blot assay and quantitative analysis of integrated optical density of PI3K/Akt signaling proteins. Data are presented as mean ± SD. The experiments were repeated three times. ††*P* < 0.01, *vs.* control group; §§*P* < 0.01, *vs.* model group; △ *P* < 0.05, △△ *P* < 0.01, *vs.* BG group (one-way analysis of variance followed by the least significant difference *post hoc* test). BG: Baicalin; LY: LY294002, an inhibitor of PI3K; NF-κB: nuclear factor-κB; PI3K/Akt: phosphatidylinositol 3-kinase/protein kinase B; ZO-1: zonula occluden-1.

Research Article

Discussion

In recent years, the neuroprotective effects of extracts and active ingredients in Scutellariae Radix have been reported in Parkinson's disease, Alzheimer disease, cerebral ischemia, and SCI (Putteeraj et al., 2018; Sowndhararajan et al., 2018). The mechanisms involve anti-apoptosis, anti-inflammation, anti-oxidative stress, anti-excitotoxicity, ameliorated BBB disruption, attenuated mitochondrial dysfunction, promoted neurogenesis, and cell differentiation (Putteeraj et al., 2018; Sowndhararajan et al., 2018). As a well-acknowledged active ingredient in Scutellariae Radix, BG is also the one that has been the most studied. In the field of SCI treatment, BG has been reported to significantly promote motor function recovery of the posterior limb, and to reverse the changes in the trends of apoptosis-related proteins, inflammatory cytokines, and NF-κB pathway proteins in spinal cord, including Bax, Bcl-2, Caspase-3, tumor necrosis factor-α, IL-1β, IL-6, NF-κB p65, NF-κB p50, p-IκBα, and IKKα (Cao et al., 2010; Kang et al., 2018). In our experiment, results were accordant with previous reports and these effects of BG were confirmed.

Disruption of the BSCB and blood-brain barrier is common in several neurodegenerative diseases and CNS traumatic injury, including SCI (Winkler et al., 2014; Kumar et al., 2017). Maintenance of BSCB integrity is crucial for SCI recovery (Cao et al., 2010; Garcia et al., 2016). In our experiment, BG distinctly restored the BSCB both *in vivo* and *in vitro*, which was consistent with previous research. In Cao's study, BG (100 mg/kg, intraperitoneal injection) significantly decreased BSCB permeability (EB leakage) and water content of the spinal cord after SCI (Cao et al., 2010). Zhu et al. (2012) established an oxygen and glucose deprivation model of primary brain microvascular endothelial cells (BMVECs). After incubation with BG (5, 10, or 20 μg/mL) for 24 hours, increases in BMVEC permeability was significantly reversed in a dose-dependent manner, as indexed by trans-endothelial electrical resistance and horseradish peroxidase leakage, as well as protein and mRNA expression of ZO-1 and claudin-5 (Zhu et al., 2012). Similar results were observed *in vivo*. In a study by Tu et al. (2011), treatment with BG (100 mg/kg, 2 and 12 hours) decreased brain edema and endogenous IgG-positive regions and increased occludin in a rat model of permanent middle cerebral artery occlusion. Along with these past results, our experiment verified the restorative effect of BG on the integrity of the BSCB, especially on TJ proteins.

However, we note one inconsistency between our rat model and cell model experiments. When examining the anti-apoptotic effects of BG, we observed that increased NF-κB expression after SCI and could be reversed by BG *in vivo*. However, NF-κB expression decreased in the excitotoxicity model of SH-SY5Y cells. Furthermore, this effect was also reversed by BG, but could not be blocked by LY294002. Why did the results for NF-κB protein expression differ between the *in vivo* and *in vitro* experiments? The CNS is mainly composed of neurons and glia (astrocytes, oligodendrocytes, microglia, and ependymal cells). Previous studies have indicated that NF-κB signaling may play a beneficial or detrimental role, depending on the cell type where it is expressed and the nature of the trauma (Kaltschmidt and Kaltschmidt, 2015; Dresselhaus et al., 2018). Under normal physiological conditions, NF-κB signaling in neurons can promote synapse growth, enhance synaptic activity, and facilitate neuronal survival (Brambilla et al., 2005; Schmeisser et al., 2012). In contrast, in neurodegenerative diseases and traumatic injury, NF-κB signaling in astrocytes contributes to pro-inflammatory responses, and inhibition of NF-κB in astrocytes can promote functional recovery. Similarly, activation of NF-κB signaling in microglia can result in an overproduction of inflammatory mediators (NO, IL-1β, tumor necrosis factor-α),

and consequently exacerbate neuronal cell death (Brambilla et al., 2009, 2012; Li et al., 2019a). Broadly summarized, NF-κB signaling plays a beneficial role primarily in neurons, while it produces harmful effects in CNS glia. In our study, the *in vitro* experiment was conducted in SH-SY5Y cells, which is a well-recognized neuronal cell model. The *in vitro* decrease in NF-κB expression of SH-SY5Y cells treated with Glu was reversed by BG, indicating a protective effect. In the *in vivo* experiment, the final result of NF-κB expression was a composite of NF-κB expressions in multiple types of cells. Thus, we measured the net change in neurons and glia, and the change in glia dominated. However, more work is needed to verify this hypothesis. Comparative works in different types of cells are necessary to investigate NF-κB signaling after SCI.

As a high-profile signaling pathway, PI3K/Akt controls various cellular events, including proliferation, apoptosis, and stress. Bax and Bcl-2 are two crucial proteins downstream from PI3K/Akt, which are closely related to apoptosis. In our experiment, p-PI3K, p/pan PI3K, p-Akt, p/pan-Akt, and Bcl-2 decreased, while Bax and Caspase-3 increased in the excitotoxicity model of SH-SY5Y cells. These results support those from previous reports (Yang et al., 2013; Cheng et al., 2016). BG significantly promoted PI3K and Akt phosphorylation, thus increasing Bcl-2, as well as decreasing Bax and Caspase-3. Blocking these findings with LY294002 verified the effect of BG on neuronal apoptosis. However, the role of the PI3K/AKT pathway is not limited to controlling apoptosis. It is also involved in autophagy. By degrading damaged organelles or pathological proteins via lysosomes, autophagy plays important roles in maintaining cellular homoeostasis. In the nervous system, constitutive autophagy is indispensable in preventing neuronal degeneration. Inhibition of autophagy by genetic elimination induced neuronal degeneration in Purkinje cells of mouse cerebellum, as well as other neurons in different brain regions (Yang et al., 2013; Zhao et al., 2015). In treating SCI, autophagy was thought to help stabilize neuronal microtubules by degrading a microtubule-destabilizing protein (superior cervical ganglia protein 10) in cultured neurons. In the *in vivo* experiment, treatment with a specific autophagy-inducing peptide (Tat-beclin1) attenuated axon retraction, promoted axon regeneration, and improved locomotor functional recovery in SCI mice. Autophagy also prevented the loss of TJ and adherens junction proteins, thus playing a beneficial role in BSCB integrity after SCI (Zhou et al., 2017; Li et al., 2019b). To sum up, the PI3K/Akt signaling pathway plays a critical part in neuronal apoptosis and autophagy, which are closely related to BSCB restoration after SCI. BG has been shown to positively affect BSCB permeability, TJ proteins loss, and neuronal apoptosis. Therefore, more attention should be paid on the effects of BG on neuronal autophagy, as well as crosstalk between apoptosis and autophagy.

In conclusion, our present study demonstrated that administering BG improved functional recovery of the posterior limb, restored BSCB integrity, and alleviated apoptosis in a rat model of SCI. The *in vitro* experiment showed that BG rescued TJ protein loss and reduced neuronal apoptosis through activation of the PI3K/Akt signaling pathway. These results suggest that therapies targeting BSCB disruption and/or apoptosis might be promising areas of research for treating SCI. Because of the satisfactory therapeutic effect in rats, BG is expected to be developed as a potential drug against SCI. Thus, more work needs to be done to investigate the underlying mechanism.

Research Article

References

Ahuja CS, Wilson JR, Nori S, Kotter MRN, Druschel C, Curt A, Fehlings MG (2017) Traumatic spinal cord injury. Nat Rev Dis Primers 3:17018.

Bartanusz V, Jezova D, Alajajian B, Digicaylioglu M (2011) The blood-spinal cord barrier: morphology and clinical implications. Ann Neurol 70:194-206.

Basso DM, Beattie MS, Bresnahan JC (1995) A sensitive and reliable locomotor rating scale for open field testing in rats. J Neurotrauma 12:1-21.

Brambilla R, Dvoriantchikova G, Barakat D, Ivanov D, Bethea JR, Shestopalov VI (2012) Transgenic inhibition of astroglial NF-κB protects from optic nerve damage and retinal ganglion cell loss in experimental optic neuritis. J Neuroinflammation 9:213.

Brambilla R, Hurtado A, Persaud T, Esham K, Pearse DD, Oudega M, Bethea JR (2009) Transgenic inhibition of astroglial NF-kappa B leads to increased axonal sparing and sprouting following spinal cord injury. J Neurochem 110:765-778.

Brambilla R, Bracchi-Ricard V, Hu WH, Frydel B, Bramwell A, Karmally S, Green EJ, Bethea JR (2005) Inhibition of astroglial nuclear factor kappaB reduces inflammation and improves functional recovery after spinal cord injury. J Exp Med 202:145-156.

Brotfain E, Gruenbaum SE, Boyko M, Kutz R, Zlotnik A, Klein M (2016) Neuroprotection by estrogen and progesterone in traumatic brain injury and spinal cord injury. Curr Neuropharmacol 14:641-653.

Cao Y, Li G, Wang YF, Fan ZK, Yu DS, Wang ZD, Bi YL (2010) Neuroprotective effect of baicalin on compression spinal cord injury in rats. Brain Res 1357:115-123.

Cheng Q, Meng J, Wang XS, Kang WB, Tian Z, Zhang K, Liu G, Zhao JN (2016) G-1 exerts neuroprotective effects through G protein-coupled estrogen receptor 1 following spinal cord injury in mice. Biosci Rep 36:e00373.

China Pharmacopoeia Commission (2020) Chinese pharmacopoeia. Beijing: China Medical Science Press.

Coisne C, Engelhardt B (2011) Tight junctions in brain barriers during central nervous system inflammation. Antioxid Redox Signal 15:1285-1303.

Dresselhaus EC, Boersma MCH, Meffert MK (2018) Targeting of NF-κB to dendritic spines is required for synaptic signaling and spine development. J Neurosci 38:4093-4103.

Fang J, Wang H, Zhou J, Dai W, Zhu Y, Zhou Y, Wang X, Zhou M (2018) Baicalin provides neuroprotection in traumatic brain injury mice model through Akt/Nrf2 pathway. Drug Des Devel Ther 12:2497-2508.

Garcia E, Aguilar-Cevallos J, Silva-Garcia R, Ibarra A (2016) Cytokine and growth factor activation in vivo and in vitro after spinal cord injury. Mediators Inflamm 2016:9476020.

Jin X, Liu MY, Zhang DF, Zhong X, Du K, Qian P, Yao WF, Gao H, Wei MJ (2019) Baicalin mitigates cognitive impairment and protects neurons from microglia-mediated neuroinflammation via suppressing NLRP3 inflammasomes and TLR4/NF-κB signaling pathway. CNS Neurosci Ther 25:575-590.

Kaltschmidt B, Kaltschmidt C (2015) NF-kappaB in long-term memory and structural plasticity in the adult mammalian brain. Front Mol Neurosci 8:69.

Kang S, Liu S, Li H, Wang D, Qi X (2018) Baicalin effects on rats with spinal cord injury by anti-inflammatory and regulating the serum metabolic disorder. J Cell Biochem 119:7767-7779.

Koehn LM (2020) ABC efflux transporters at blood-central nervous system barriers and their implications for treating spinal cord disorders. Neural Regen Res 15:1235-1242.

Kumar H, Ropper AE, Lee SH, Han I (2017) Propitious therapeutic modulators to prevent blood-spinal cord barrier disruption in spinal cord injury. Mol Neurobiol 54:3578-3590.

Lee JY, Kim HS, Choi HY, Oh TH, Ju BG, Yune TY (2012) Valproic acid attenuates blood-spinal cord barrier disruption by inhibiting matrix metalloprotease-9 activity and improves functional recovery after spinal cord injury. J Neurochem 121:818-829.

Li H, Zhang X, Qi X, Zhu X, Cheng L (2019a) Icariin inhibits endoplasmic reticulum stress-induced neuronal apoptosis after spinal cord injury through modulating the PI3K/AKT signaling pathway. Int J Biol Sci 15:277-286.

Li LH, Jia AM, Yang MH, Liu Z, Wang LH, Jiang H, Qiu Y (2018) Effect of baicalin on human periodontal ligament fibroblasts and the underlying molecular mechanism. Zhongguo Zuzhi Gongcheng Yanjiu 22:4475-4480.

Li Y, Liu T, Li Y, Han D, Hong J, Yang N, He J, Peng R, Mi X, Kuang C, Zhou Y, Han Y, Shi C, Li Z, Guo X (2020) Baicalin ameliorates cognitive impairment and protects microglia from LPS-induced neuroinflammation via the SIRT1/HMGB1 pathway. Oxid Med Cell Longev 2020:4751349.

Li Z, Chen T, Cao Y, Jiang X, Lin H, Zhang J, Chen Z (2019b) Pros and cons: autophagy in acute spinal cord injury. Neurosci Bull 35:941-945.

Liu J, Zhang T, Wang Y, Si C, Wang X, Wang RT, Lv Z (2020) Baicalin ameliorates neuropathology in repeated cerebral ischemia-reperfusion injury model mice by remodeling the gut microbiota. Aging (Albany NY) 12:3791-3806.

Ozturk AM, Sozbilen MC, Sevgili E, Dagci T, Özyalcin H, Armagan G (2018) Epidermal growth factor regulates apoptosis and oxidative stress in a rat model of spinal cord injury. Injury 49:1038-1045.

Putteeraj M, Lim WL, Teoh SL, Yahaya MF (2018) Flavonoids and its neuroprotective effects on brain ischemia and neurodegenerative diseases. Curr Drug Targets 19:1710-1720.

Quadri SA, Farooqui M, Ikram A, Zafar A, Khan MA, Suriya SS, Claus CF, Fiani B, Rahman M, Ramachandran A, Armstrong IIT, Taqi MA, Mortazavi MM (2020) Recent update on basic mechanisms of spinal cord injury. Neurosurg Rev 43:425-441.

Sandhir R, Gregory E, He YY, Berman NE (2011) Upregulation of inflammatory mediators in a model of chronic pain after spinal cord injury. Neurochem Res 36:856-862.

Schmeisser MJ, Baumann B, Johannsen S, Vindedal GF, Jensen V, Hvalby Ø C, Sprengel R, Seither J, Maqbool A, Magnutzki A, Lattke M, Oswald F, Boeckers TM, Wirth T (2012) IκB kinase/nuclear factor κB-dependent insulin-like growth factor 2 (Igf2) expression regulates synapse formation and spine maturation via Igf2 receptor signaling. J Neurosci 32:5688-5703.

Sowndhararajan K, Deepa P, Kim M, Park SJ, Kim S (2018) Neuroprotective and cognitive enhancement potentials of baicalin: a review. Brain Sci 8:104.

Tu XK, Yang WZ, Liang RS, Shi SS, Chen JP, Chen CM, Wang CH, Xie HS, Chen Y, Ouyang LQ (2011) Effect of baicalin on matrix metalloproteinase-9 expression and blood-brain barrier permeability following focal cerebral ischemia in rats. Neurochem Res 36:2022-2028.

Winkler EA, Sengillo JD, Sagare AP, Zhao Z, Ma Q, Zuniga E, Wang Y, Zhong Z, Sullivan JS, Griffin JH, Cleveland DW, Zlokovic BV (2014) Blood-spinal cord barrier disruption contributes to early motor-neuron degeneration in ALS-model mice. Proc Natl Acad Sci U S A 111:E1035-1042.

Wu KL, Chan SH, Chao YM, Chan JY (2003) Expression of pro-inflammatory cytokine and caspase genes promotes neuronal apoptosis in pontine reticular formation after spinal cord transection. Neurobiol Dis 14:19-31.

Yang Y, Coleman M, Zhang L, Zheng X, Yue Z (2013) Autophagy in axonal and dendritic degeneration. Trends Neurosci 36:418-428.

Ye LX, An NC, Huang P, Li DH, Zheng ZL, Ji H, Li H, Chen DQ, Wu YQ, Xiao J, Xu K, Li XK, Zhang HY (2021) Exogenous platelet-derived growth factor improves neurovascular unit recovery after spinal cord injury. Neural Regen Res 16:765-771.

Zhang CY, Zeng MJ, Zhou LP, Li YQ, Zhao F, Shang ZY, Deng XY, Ma ZQ, Fu Q, Ma SP, Qu R (2018) Baicalin exerts neuroprotective effects via inhibiting activation of GSK3β/NF-κB/NLRP3 signal pathway in a rat model of depression. Int Immunopharmacol 64:175-182.

Zhang Q, Liu X, Yan L, Zhao R, An J, Liu C, Yang H (2019) Danshen extract (Salvia miltiorrhiza Bunge) attenuate spinal cord injury in a rat model: A metabolomic approach for the mechanism study. Phytomedicine 62:152966.

Zhao YG, Sun L, Miao G, Ji C, Zhao H, Sun H, Miao L, Yoshii SR, Mizushima N, Wang X, Zhang H (2015) The autophagy gene Wdr45/Wipi4 regulates learning and memory function and axonal homeostasis. Autophagy 11:881-890.

Zhou Y, Wu Y, Liu Y, He Z, Zou S, Wang Q, Li J, Zheng Z, Chen J, Wu F, Gong F, Zhang H, Xu H, Xiao J (2017) The cross-talk between autophagy and endoplasmic reticulum stress in blood-spinal cord barrier disruption after spinal cord injury. Oncotarget 8:1688-1702.

Zhu H, Wang Z, Xing Y, Gao Y, Ma T, Lou L, Lou J, Gao Y, Wang S, Wang Y (2012) Baicalin reduces the permeability of the blood-brain barrier during hypoxia in vitro by increasing the expression of tight junction proteins in brain microvascular endothelial cells. J Ethnopharmacol 141:714-720.